Contents lists available at ScienceDirect

Journal of Pharmaceutical Analysis

journal homepage: www.elsevier.com/locate/jpa

Original article

Simultaneously quantifying hundreds of acylcarnitines in multiple biological matrices within ten minutes using ultrahigh-performance liquid-chromatography and tandem mass spectrometry

Jingxian Zhang [a,1], Qinsheng Chen [a,1], Lianglong Zhang [a], Biru Shi [a], Men Yu [b], Qingxia Huang [a,**], Huiru Tang [a,*]

[a] State Key Laboratory of Genetic Engineering, School of Life Sciences, Human Phenome Institute, Zhangjiang Fudan International Innovation Center, Metabonomics and Systems Biology Laboratory at Shanghai International Centre for Molecular Phenomics, Zhongshan Hospital, Fudan University, Shanghai, 200032, China
[b] Wuhan Laboratory for Shanghai Metabolome Institute (SMI) Ltd., Wuhan, 430000, China

ABSTRACT

Acylcarnitines are metabolic intermediates of fatty acids and branched-chain amino acids having vital biofunctions and pathophysiological significances. Here, we developed a high-throughput method for quantifying hundreds of acylcarnitines in one run using ultrahigh performance liquid chromatography and tandem mass spectrometry (UPLC-MS/MS). This enabled simultaneous quantification of 1136 acylcarnitines (C0–C26) within 10-min with good sensitivity (limit of detection < 0.7 fmol), linearity (correlation coefficient > 0.992), accuracy (relative error < 20%), precision (coefficient of variation (CV), CV < 15%), stability (CV < 15%), and inter-technician consistency (CV < 20%, $n = 6$). We also established a quantitative structure-retention relationship (goodness of fit > 0.998) for predicting retention time (t_R) of acylcarnitines with no standards and built a database of their multiple reaction monitoring parameters (t_R, ion-pairs, and collision energy). Furthermore, we quantified 514 acylcarnitines in human plasma and urine, mouse kidney, liver, heart, lung, and muscle. This provides a rapid method for quantifying acylcarnitines in multiple biological matrices.

© 2023 The Authors. Published by Elsevier B.V. on behalf of Xi'an Jiaotong University. This is an open access article under the CC BY-NC-ND license (http://creativecommons.org/licenses/by-nc-nd/4.0/).

1. Introduction

Acylcarnitines are esters of carnitine (3-hydroxy-4-trimethylaminobutyric acid) derived from fatty-acids and branched-chain amino acids in mitochondria, peroxisome, and endoplasmic reticulum [1–10]. Although several thousand acylcarnitine species were predicted to be possibly present in the human samples [9], only a few hundred acylcarnitines were collectively reported with their acyl-chains containing 2–28 carbons (C2–C28) [11,12]. Based on the acyl-chain length, they can be categorized as short-chain (C2–5), medium-chain (C6–12), long-chain (C13–20), and very-long chain (>C20) acylcarnitines [8–10]

(Fig. 1). The acyl-chains may also contain hydroxyl, carboxylic, and side-chain methyl groups so that these subgroups can be termed as hydroxylated, carboxylated, and branched-chain acylcarnitines, respectively [9,10]. More recently, some acylcarnitines conjugated with numerous hydrophilic compounds including amino acids, glucuronic acid, and sulfoacid (Fig. 1) were discovered though only in urine so far which were probably derived from phase II biotransformation [12].

These acylcarnitines play many vital roles including metabolic homeostasis of lipids and amino acids, fatty acid transportation, and host-microbial symbiosis [3–10]. Numerous acylcarnitines have been reported as biomarkers for type-2 diabetes, cardiovascular diseases, Alzheimer's disease, non-alcoholic fatty liver disease, tumors, and inborn errors of metabolism [13–21]. However, the functions of branched-chain, hydroxylated, carboxylated, and conjugated acylcarnitines are far from fully understood. Conceivably, simultaneous quantification of all these acylcarnitines is the prerequisite to effectively investigate their diverse functions thus reveal acylcarnitine-related molecular phenotypes of biological
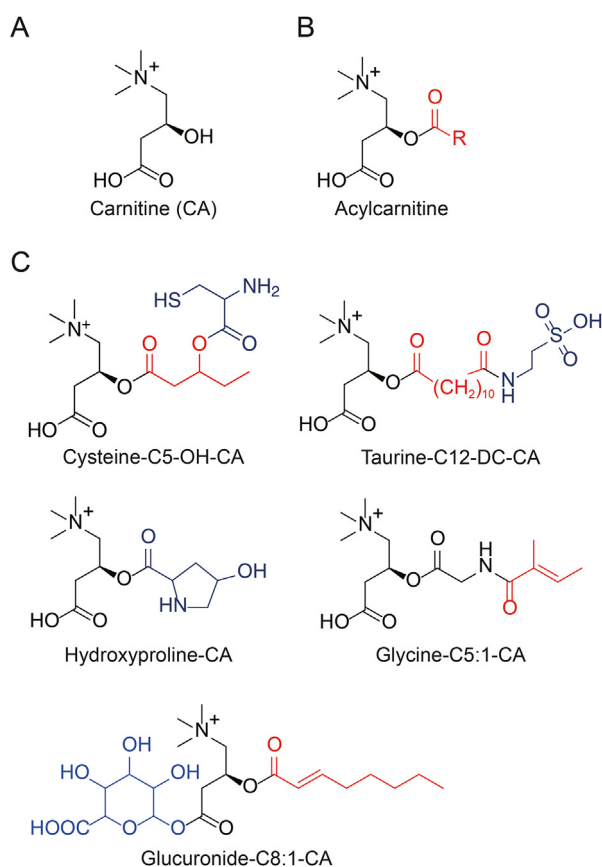
Fig. 1. Structure of carnitines detected in biological samples. (A) Carnitine (CA). (B) Typical acylcarnitines whose acyl-group R (C2–C26) may contain straight chains and branched-chains, double bonds, hydroxyl (OH), and carboxyl (DC) groups. (C) Some typical conjugated acylcarnitines.

systems. Unfortunately, such analysis is nontrivial with huge diversity for the structural and physiochemical properties of acylcarnitines. Concurrent high-coverage and high-throughput quantification of acylcarnitines is still needed especially for large cohort population studies.

Ultrahigh performance liquid chromatography coupled with mass spectrometry (UPLC-MS) has shown great potentials for simultaneous detection and quantification of acylcarnitines [11,12,22–24], whilst flow injection MS methods [25] cannot distinguish isomers. For example, 733 acylcarnitines in the pooled samples from rat liver tissue, human plasma, and urine were reportedly detected with UPLC-coupled high-resolution mass spectrometry (HRMS) although the method required more than 10 runs (with 19 min each) [11]. A recent HRMS study also reported coverage of 586 acylcarnitines and 125 conjugated acylcarnitines from human urine [12] with 108 individual runs (22 min each) but without quantitative data. For simultaneous quantifications, HRMS is limited by its scanning-speed and dynamic range hence accuracy for low abundant acylcarnitines such as those having poly-unsaturated, hydroxylated, and carboxylated acyl-chains [24]. UPLC-MS/MS in scheduled multiple reaction monitoring (MRM) mode should be the best choice. However, the reported UPLC-MS/MS methods either had thermal instability problems or limited coverage, throughput or isomer differentiability [26–30]. Even with the combination of reversed- and normal-phase liquid chromatography (LC), such LC-MS/MS method could only quantify 117 acylcarnitines in biofluids with a 26-min run [29]. All the reported LC-MS/MS methods covered only a few hydroxylated and carboxylated acylcarnitines with no conjugated acylcarnitines [9].

One of the bottlenecks for high-coverage LC-MS/MS quantification of acylcarnitines is the lack of standards to reliably obtain the retention time (t_R) of all possible acylcarnitines for scheduled MRM analysis. For hundreds of acylcarnitines reportedly detected, only dozens of them have commercial standards. Under such circumstances, reliable modelling for quantitative structure-retention relationship (QSRR) becomes helpful to predict their t_R [31,32] for setting up the MRM-needed time-windows and to assist identification. Previous studies have already shown potential linear relationship between t_R and some structural descriptors for acylcarnitines [11,30,33]. Unfortunately, these required massive calculation resources and gave no information for the t_R dependence on functional groups. Understandably, the retention behaviors of acylcarnitines collectively depend on structural characteristics of their acyl-chains including the number of carbons, double-bonds, side-chains, hydroxyl and carboxyl groups, and their positions. So far, however, the best such study has considered only the number of carbon atoms and double bonds in acyl-chains with several linear models constructed for different classes of acylcarnitines [34]. A unified QSRR model for demanded structural features has not been reported so far, to the best of our knowledge.

Here, we developed an MRM-based sensitive UPLC-MS/MS method for simultaneous quantification of all identifiable acylcarnitines in biofluids and tissues with a single 10-min run. We also built a QSRR model for predicting acylcarnitine t_R values with their seven structural features and constructed a database of MRM parameters (t_R, MRM ion-pairs, and collision energy) for 1136 acylcarnitines detected in literatures and with UPLC-based quadrupole time-of-flight MS (UPLC-QTOFMS) in this study. We further quantified acylcarnitines in two typical human biofluids (plasma and urine) and five typical tissues of animal model to reveal their molecular phenotypic characteristics.

2. Materials and methods

2.1. Chemicals

HPLC grade methanol (MeOH), isopropyl alcohol (IPA), and dichloromethane were obtained from Merck (Darmstadt, Germany) whereas acetonitrile (ACN), formic acid, and acetic acid were purchased from Sigma-Aldrich (St. Louis, MO, USA). Ultrapure water (H_2O) was obtained from a Milli-Q system (Millipore, Billerica, MA, USA). 49 acylcarnitine standards and 26 deuterated ones as internal standards (IS) were purchased from commercial sources with detailed information listed in Table S1.

2.2. Collection of biological samples

Human plasma and urine were obtained from Chinese adult volunteers recruited for the Human Phenome Project which was approved by the Ethic Committee of Fudan University (Approval No.: FE21087) with informed consent from all participants. Human lung cancer cell lines (A549, 16HBE) were obtained from China Center for Type Culture Collection. The New Zealand rabbit liver and five tissue samples of C57BL/6 mice were collected according to the National Guidelines for Experimental Animal Welfare (Ministry of Science and Technology of China, 2006). All biological samples were snap-frozen with liquid-nitrogen and stored at −80 °C until further analysis.

2.3. Preparation of stock and working solutions

Each acylcarnitine standard was dissolved in MeOH or CH_2Cl_2:MeOH (3:2, V/V) to prepared individual stock solution

(1–15 mM). These solutions were mixed, dried with nitrogen-gas, and reconstituted into aqueous MeOH (90%, *V/V*) to obtain the stock solution of acylcarnitine mixture. This mixture solution was then sequentially diluted to obtain 13 solutions for constructing calibration curves (Levels 1–13, Tables S2–S4). The mixture of 26 deuterated acylcarnitines in 90% (*V/V*) aqueous MeOH was used as IS.

2.4. Preparation of biological samples for analysis of acylcarnitines

For UPLC-QTOFMS analysis, acylcarnitines were extracted from multiple biological matrices including rabbit liver tissue, human plasma, urine, and cells as described in the Supplementary data. For quantification of acylcarnitines in biofluids and tissues, analytes were extracted with an optimized procedure. Briefly, 20 μL of each human plasma or urine was mixed with 500 μL pre-cooled IPA containing 0.5% (*V/V*) acetic acid, 20 μL mixed IS solution, and 30 μL water, and sonicated in an ice-bath for 5 min. After centrifugation (4 °C, 16,000 *g*) for 10 min, 520 μL of supernatant was obtained. The above procedure was repeated once more and resultant 2 supernatants were combined and dried with nitrogen-gas. Each tissue sample (10 mg) was added with 400 μL pre-cooled IPA containing 0.5% (*V/V*) acetic acid, 20 μL mixed IS, and 30 μL water, and then homogenized with a tissuelyser (20 Hz) for 3 min to obtain supernatant after 10-min centrifugation (4 °C, 16,000 *g*). This extraction was repeated two more times and three resultant supernatants were pooled and dried. These dried extracts were individually reconstituted into 90% (*V/V*) MeOH (40 μL) for UPLC-MS/MS analysis.

2.5. UPLC-MS analysis

A ZenoTOF 7600 and TripleTOF 5600 plus (SCIEX, Chromos, Singapore) coupled to a Shimazu UPLC system were used in the information-dependent acquisition (IDA) mode (Supplementary data) to detect acylcarnitines and their fragment ions in multiple biological samples. A QTRAP 6500 Plus (SCIEX) coupled to two Shimadzu Nexera UPLC systems (Kyoto, Japan) was used for simultaneous quantification of acylcarnitines with scheduled MRM. Data were acquired and processed with Analyst and OS (v1.7, SCIEX). After comprehensive optimization of various C_{18} columns and chromatographic conditions, the best performer Agilent ZORBAX Eclipse Plus C_{18} column (2.1 mm × 100 mm, 1.8 μm; Santa Clara, CA, USA) was chosen at 40 °C with 0.5 μL of sample injection. H_2O and ACN (both containing 0.1% (*V/V*) formic acid) were used as mobile phase A and B, respectively, with elution gradients listed in Table S5. The dual-column-switching mode (Fig. S1) with Multiplexing (MPX) software was used to double throughput. By using acylcarnitine standards, mass spectrometric parameters were optimized including ionspray voltage, curtain gas, ion source temperature, collision energy, and declustering potential (Supplementary data). Collision energy values were further adjusted to ensure simultaneous quantification of all acylcarnitines in a single run for all biological matrices (Table S6).

2.6. Method validation

Method validation was conducted for sensitivity, linearity, accuracy, precision, stability, and inter-technician consistency. Linearity and sensitivity were assessed using acylcarnitine standards with variable concentration and IS. The limit of detection (LOD) was obtained as the amount of analytes on column at the signal-to-noise ratio (S/N) of 3 whereas the low limit of quantification (LLOQ) was obtained from the lowest amount in calibration curve according to the U.S. Food and Drug Administration guideline [35].

Accuracy, precision, and stability were evaluated with plasma, urine, and liver samples at three different concentration levels (L3, L5, and L7). Accuracy was assessed with relative error (RE) at high, medium, and low levels whilst precision was assessed with the coefficient of variation (CV) for the intra- and inter-day measurements. Stability was assessed with extracted samples stored at −4 °C for 24 h and at −80 °C for 72 h. Inter-technician consistency was evaluated using the same batch of plasma samples (*n* = 6) with the independent results from three different technicians.

2.7. QSRR and MRM-parameter database

The QSRR model was built with multivariate polynomial regression approach [36,37] using experimental data from 45 known acylcarnitines (Table S1) containing saturated (18), unsaturated (12), hydroxylated (9), and dicarboxylic (6) acyl-chains. LM functions in R software package (v4.1.0) was used to optimize models with t_R dependence on various structural features for acyl chains with stepwise regression and full subset regression. These features included the number of carbon atoms (*c*), branched-chain methyl groups (*b*), carbon-carbon double bonds (*d*), hydroxyl groups (*h*), carboxyl groups (*j*), position of branched-chain (*p*), and double bonds (*q*). 10-fold cross-validation was conducted to obtain the optimized model with minimum prediction error and favorable adjusted-goodness of fit (R^2_a, Eq. (1)). Based on the experimental and calculated t_R results, mean absolute error (MAE, Eq. (2)) and Pearson correlation coefficient (r^2) were used to assess the overall performance of model.

$$R_a^2 = 1 - \frac{\left(1 - \frac{\sum_{i=1}^{N}(\widehat{y_i} - \overline{y})^2}{\sum_{i=1}^{N}(y_i - \overline{y})^2}\right)(n-1)}{n - m - 1} \qquad \text{(Eq. 1)}$$

$$\text{MAE} = \frac{\sum_{i=1}^{N}|y_i - \widehat{y_i}|}{n} \qquad \text{(Eq. 2)}$$

where y_i, $\widehat{y_i}$, $\overline{y}$ denote the experimental, predicted, and mean of experimental and predicted values, respectively, whilst *n* and *m* denote the number of samples and variables. The predicted t_R results were used for MRM when acylcarnitine standards were not available. A database covering 1136 acylcarnitines was constructed (Table S7) including molecular formulae, four MRM ion-pairs, collision energy, t_R, and MRM detection window ($t_R ± 1$ min).

3. Results and discussion

3.1. Detection of acylcarnitines in multiple biological matrices with UPLC-QTOFMS

Although thousands of acylcarnitines have been suggested in the Human Metabolome Database, so far, only dozens of them have experimental mass spectrometric data due to limited standards available. To obtain such data, we employed UPLC-QTOFMS in full-scan and IDA modes to detect all possible acylcarnitines present in multiple biological matrices including biofluids, cells, and tissues. Chromatographic parameters were systematically optimized including column, temperature, elution gradients, flow-rate, and injection volume to achieve maximum separation (data not shown). Since carnitine moiety has a quaternary ammonium cation, $(CH_3)_3N^+R$, with permanent charge, acylcarnitines are expected to have some unique mass spectrometric features. In the negative ion mode, all acylcarnitines gave parent ions as $[M+HCOO^--H]^-$,

fragment ions for carnitine moiety (m/z 188.0934 and 144.1042) and [FA−H]$^-$ from fatty-acid chains (Fig. S2). In the positive ion mode, in contrast, much more intense signals including parent ions [M]$^+$ due to the carnitine quaternary ammonium cations, [M−59.0735]$^+$ due to neutral loss of N(CH$_3$)$_3$, and three fragment ions from carnitine moiety (m/z 144.1019, 85.0284, and 60.0808) were observable for all acylcarnitines (Figs. 2A and S2) as reported [38−40]. All conjugated acylcarnitines gave parent ions [M]$^+$, [M−conjugator−59.0735]$^+$, and three fragment ions from carnitine moiety (Figs. 2B and S2) as reported [12,38]. Therefore, acylcarnitines and conjugated acylcarnitines were both readily identifiable collectively with their aforementioned five ions, respectively. Acylcarnitines gave the most intense fragment ion m/z 85.0284, thus MRM ion-pair [M]$^+$/85.0284 was useable for quantifying acylcarnitines (Fig. S3). In contrast, [M−conjugator−59.0735]$^+$ was a unique intense fragment ion for conjugated acylcarnitines (Fig. 2B), thus [M]$^+$/[M−conjugator−59.0735]$^+$ was employable for their quantification. Typical ions were also recorded for 26 deuterated acylcarnitines, which were commercially available and used as internal standards for quantification.

By concurrently extracting the above ions, we identified 471 acylcarnitines including 395 acylcarnitines and 76 conjugated ones from above biological matrices (rabbit liver tissue, human plasma,

urine, and cells) and their pooled samples (Fig. S4). After taking structural isomers having different retention time into consideration, the coverage of acylcarnitines having different retention time was expanded to 1136 species (Table S7) including 1124 possible species derived from these collectively reported in literatures [11,12,29,41,42]. Unambiguous identification was achieved for acylcarnitine isomers having commercial standards (Tables S7 and S8) such as butyryl-carnitine (C4:0) and isobutyry-carnitine (2-M-C3:0), succinyl-carnitine (C4-DC), and methylmalonyl-carnitine (2-M-C3-DC) as well as adipoyl-carnitine (C6-DC) and 3-methylglutaryl-carnitine (3-M-C5-DC). For acylcarnitines with saturated five-carbon chains (C$_{12}$H$_{23}$NO$_4$), for instance, four isomers were detected with clearly different retention times. By using the commercially available standards, three of them were unambiguously assigned as valerylcarnitine (C5:0), 2-methylbutyryl-carnitine (2-M-C4:0), and isovalerylcarnitine (3-M-C4:0), respectively; pivaloylcarntine (2-2M-C3:0) became the only possibility for the remaining isomer and was further confirmed using its standard. Furthermore, the isomers without commercial standards were only considered as present here when detected with clearly different retention times (Table S8). They can be unambiguously identified with extensive syntheses of their standards, which is beyond the scope of this study. Nevertheless, we identified these isomers as analyte-a, analyte-b, etc. here
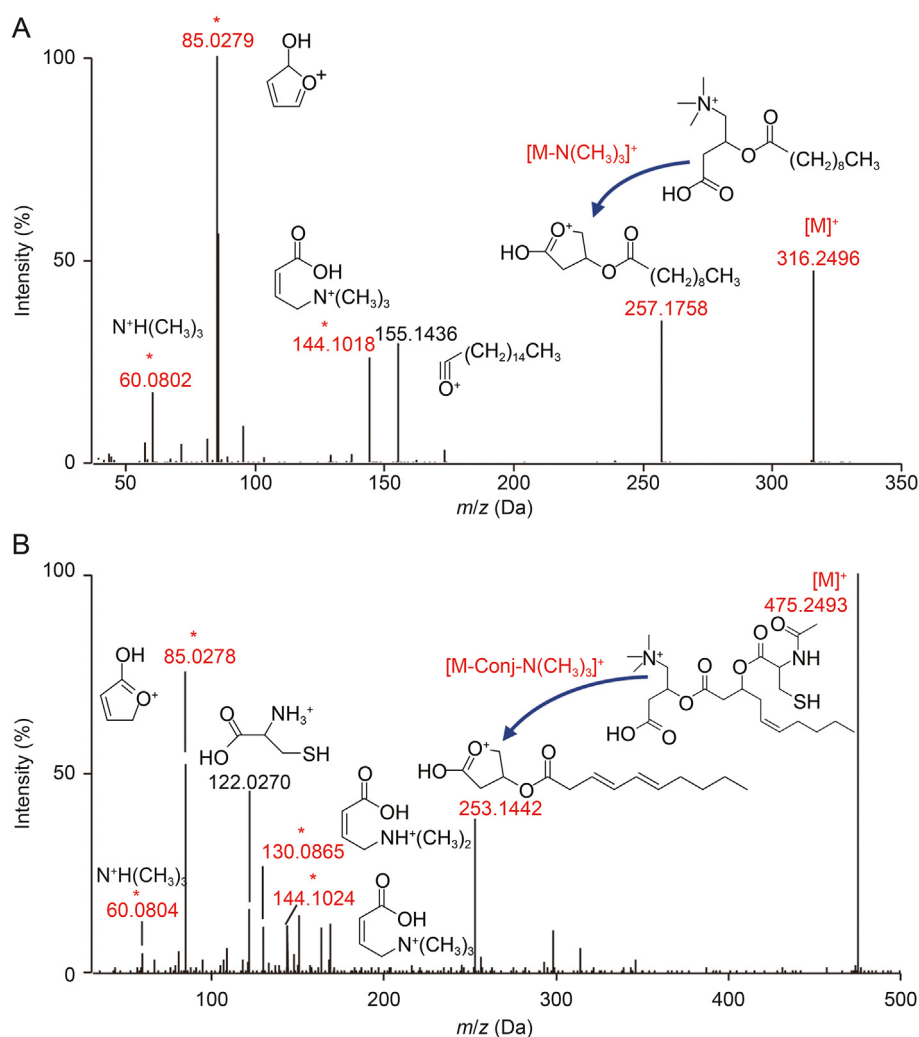

Fig. 2. Fragment assignments for (A) decanoylcarnitine (C10:0) and (B) *N*-acetylcysteine-conjugated-hydroxydecenoylcarnitine (*N*-acetylcys-C10:1-OH-CA) in the positive ion mode. * Fragment ions for carnitine moiety. Conj: conjugator.

to ensure their separate identities. For instance, five isomers were detected for acylcarnitines with saturated six-carbon chains giving same precursor and fragment ions in both Q-TOFMS and MS/MS. Hexanoyl-carnitine was unambiguously assigned (C6:0) with its standard and the other four were tentatively assigned to be C6:0-a, C6:0-b, C6:0-c, and C6:0-d (Table S8) respectively. It is conceivable that the identification of isomers can also be assisted to some extent by reliable prediction of their t_R.

3.2. QSRR and MRM parameter database

The parameters for t_R and precursor-product ion pairs for MRM transitions (MRM ion-pairs) are necessary for simultaneous quantification of all acylcarnitines in the scheduled MRM mode using UPLC-MS/MS [43]. However, only less than 50 acylcarnitines have standards available currently. Nevertheless, our t_R results of these available acylcarnitines clearly showed some dependence on their structural features (Fig. S5A) as indicated previously [44,45]. These structural features included the number of carbons, branched-chains, double-bonds, hydroxyl, carboxylic groups, and positions in their acyl-chains. With the same number of acyl-chain carbons, the presence of these groups resulted in earlier elution. Amongst four isomers of acylcarnitines with five acyl-chain carbons, for example, C5:0 had the greatest t_R followed with 3-M-C4:0, 2-M-C4:0, and then 2-2M-C3:0.

By using 45 acylcarnitine standards (Table S1) excluding carnitine and acetylcarnitine for their close-to-void elution, a unified QSRR model was built for t_R values (i.e., the model-calculated retention times (t_R^C)) obtained from our chromatographic method (including column and elution schemes) as a function of acyl-chain structural characteristics (Eq. (3)) with the fitted k_0-k_{10} data obtained (i.e., $k_0 = -0.252$, $k_1 = 8.54 \times 10^{-4}$, $k_2 = -4.82 \times 10^{-2}$, $k_3 = 1.06$, $k_4 = -0.487$, $k_5 = -0.172$, $k_6 = -1.65$, $k_7 = -1.55$, $k_8 = 0.152$, $k_9 = -1.59 \times 10^{-2}$, and $k_{10} = 7.20 \times 10^{-2}$). In the model, variables c, b, d, h, and j denote the number of acyl-chain carbon, branched-chain methyl group, carbon-carbon double-bond, hydroxyl, and carboxylic groups, respectively, whilst p and q denote the positions of the branched-chains and double-bonds.
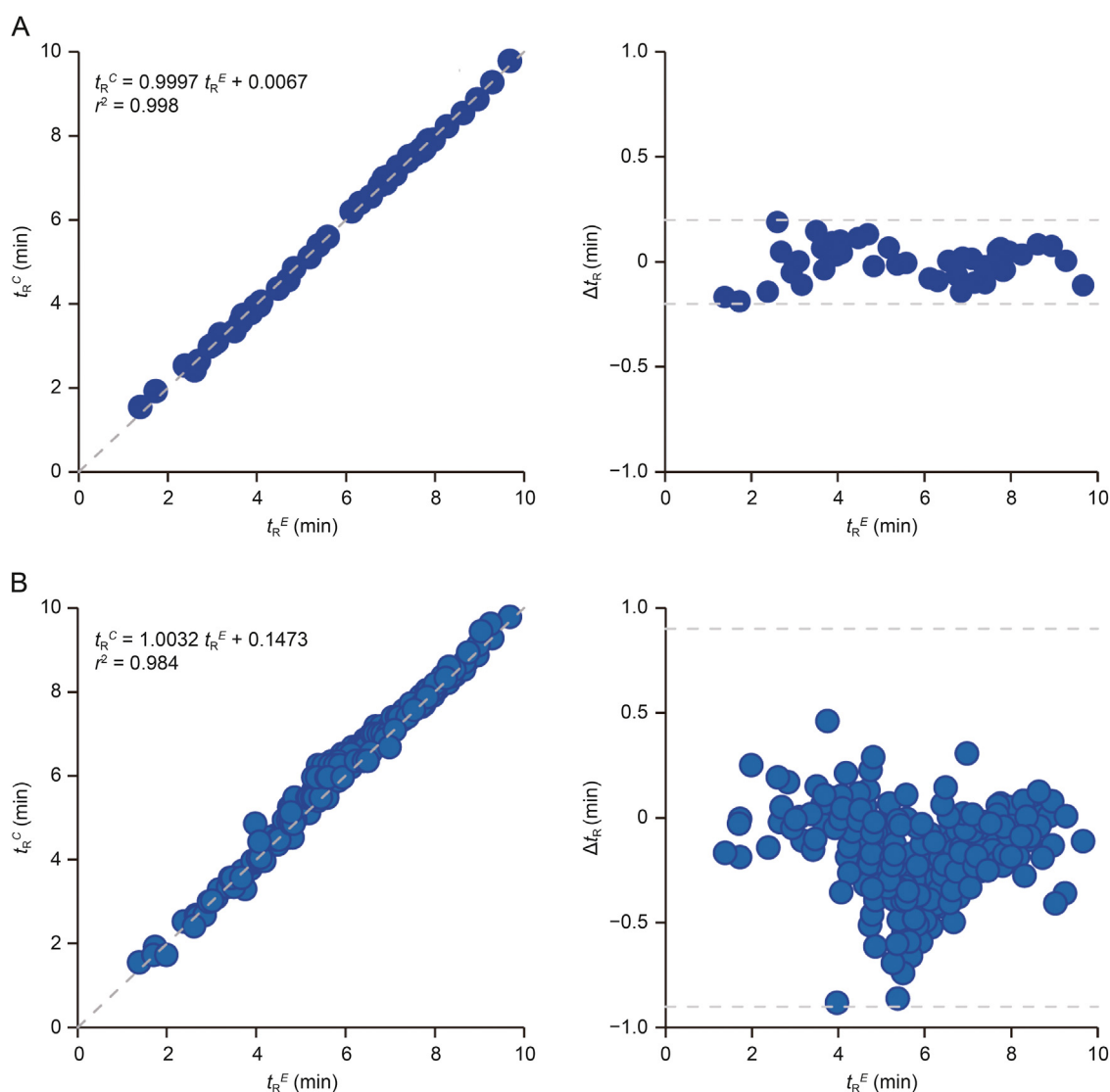

Fig. 3. Comparison of the model-calculated retention times (t_R^C) and experimental results (t_R^E) for (A) 45 acylcarnitine standards and (B) acylcarnitines detected in biological samples.

$$t_R^C = k_0 + k_1 c^3 + k_2 c^2 + k_3 c + k_4 b + k_5 d + k_6 h + k_7 j + k_8 p + k_9 q + k_{10} ch$$

<div align="right">(Eq. 3)</div>

Such a unified model could predict t_R values for all different classes of acylcarnitines with good performance ($R_a^2 > 0.998$) for chain length of C3−C26, which were only describable with multiple linear models previously [11,30,34]. The t_R^C and experimental results (t_R^E) showed excellent linear correlation (r^2, 0.998) and accuracy ($\Delta t_R < 0.20$ min and MAE < 0.07 min) for 45 acylcarnitine standards (Fig. 3A). Such t_R differences between the experimental and predicted values were 0.46 and 0.01 min for 2-2M-C3:0 and C4-DC, respectively, when using the present chromatographic method.

The model also showed good t_R^C and t_R^E correlation ($r^2 \sim 0.984$) and prediction accuracy (MAE <0.21 min and $\Delta t_R < 0.9$ min) for all 211 acylcarnitines detected here from the pooled sample having variable acyl-chain carbons, branch-chains, double-bonds, or hydroxyl or dicarboxylic groups (Fig. 3B). Even with concurrent presence of these structure features, the model showed reasonable t_R^C and t_R^E correlation ($r^2 \sim 0.956$) and accuracy (MAE < 0.25 min, $\Delta t_R < 0.9$ min) for 97% acylcarnitines identified from the pooled sample (Fig. S5B). By setting the t_R range of 2 min for MRM window, even the acylcarnitine isomers without commercial standards can be reliably covered in UPLC-MS/MS quantification. Taking all this together, we built a database of MRM parameters (t_R, MRM ion-

pairs, and collision energy) to cover 1136 acylcarnitine species with 398 formulae including acylcarnitines, conjugated ones and their isomers (Table S7). Among them, hydroxylated, unsaturated, dicarboxylated, conjugated, and saturated acylcarnitines accounted for 31.6%, 24.9%, 18.5%, 11.5%, and 7.9%, respectively; acylcarnitines with dicarboxylated chains and hydroxyl group accounted for 5.5%.

3.3. Development of quantitative method for acylcarnitines using UPLC-MS/MS

Based on the above investigations, we established an efficient method for simultaneous quantification of all possible carnitines within 10 min using UPLC-MS/MS in MRM mode. With all standards available commercially, the method showed good separation powers for acylcarnitine isomers with acyl-chains containing C0−C26 (Fig. 4), which was exemplified with resolution of 1.14−1.24 for acylcarnitine isomers with C5:0 (peaks 16−18). All deuterated standards with N-CD$_3$ (peaks 50−53 and 55−75) had similar retention times to the corresponding acylcarnitines (Fig. 4). This is in contrast to methyl-D$_3$-malonylcarnitine (peak 54) and suggests the N-CD$_3$-labeled acylcarnitines as good IS for quantifications.

Fragment ion m/z 85.0284 reached maximum with collision energy above 30 consistently for short chain (C4:0), medium chain (C10:0), long chain (C16:0), and very-long chain (C22:0) acylcarnitines hence being employable as a quantitative ion (Fig. S3). Other MS parameters were further optimized using all acylcarnitine
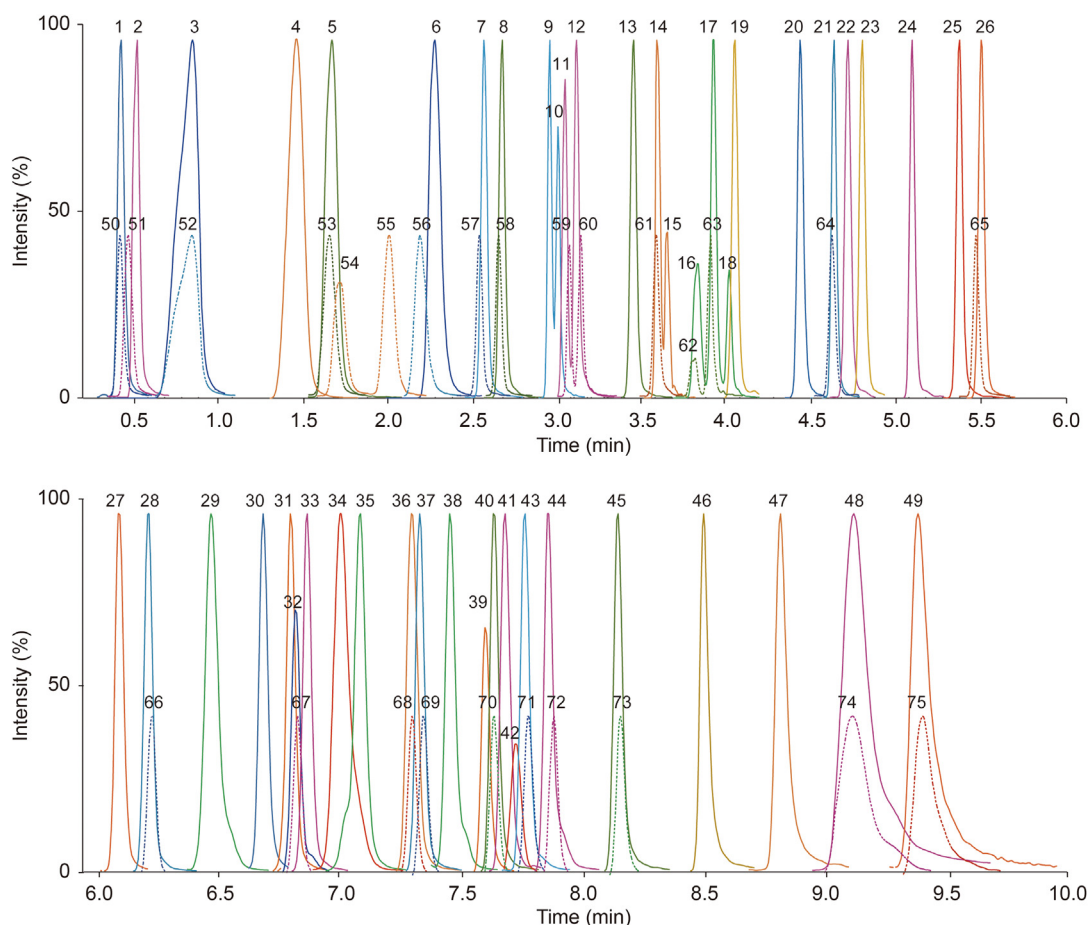

Fig. 4. Ultrahigh performance liquid chromatography and tandem mass spectrometry (UPLC-MS/MS) chromatogram (up: 0−6.0 min; bottom: 6.0−10.0 min) for 49 acylcarnitine standards (solid line) and 26 deuterated internal standards (dotted line) with keys listed in Table S1.

standards available (Fig. S6), which were used with the deuterated standards to generate calibration curves. For these without authentic standards, such MS parameters for analytes in the same subclass with the closest retention time were used and the results were considered as relative quantification. For instance, MS parameters for C10:0 were used for quantification of C9:0, whose standard was not available.

The method was further validated in terms of linearity, sensitivity, accuracy, precision, stability, and inter-technician consistency. For all acylcarnitines having authentic standards, excellent linearity ($r^2 > 0.992$) was observed with concentration over 3–4 orders of magnitude and the LOD below 0.7 fmol on column (Table S9), with the exception for only carnitine (<3.5 fmol). The method had good accuracy (RE < 20%), intra- and inter-day precision (CV < 15%), as well as stability (CV < 15%) at 4 °C (24 h) and −80 °C (72 h) for all spiked standards in plasma, liver, and urine samples (Figs. S7–S9). Acceptable inter-technician consistency (CV < 20%) was further confirmed from independent experiments conducted by three different technicians (Fig. S10). With dual-column switching (MPX mode), finally, the method was capable of quantifying 1136 carnitines within 10 min; both throughput and coverage were better than the existing methods (Table S10) [11,12,26–30].

3.4. Quantification of acylcarnitines in multiple biological matrices to characterize their molecular phenotypes

By using this method, we managed to quantify 514 acylcarnitines collectively in two typical human biofluids (plasma and urine) and five mouse tissues (kidney, liver, heart, lung, and muscle) to characterize their metabolome-based molecular phenotypes (Fig. 5 and Table S8). The results showed carnitine itself as the most abundant in all samples. However, clear acylcarnitine phenotypic differences were observable between biofluids and tissues, between two biofluids and between different tissues from the same animal (Fig. 5 and Table S8). Human urine samples contained more acylcarnitine species (421) than human plasma (149) and mouse tissues including kidney (211), liver (195), heart (189), lung (188), and muscle (169), especially conjugated acylcarnitines and these with hydroxyl and carboxylic groups (Fig. 5 and Table S8). Noticeably, some carnitine species were only detected in urine including 3-dehydrocarnitine, pivaloylcarnitine, and isomers of C6:0, C8:0, C10:0, C11:0, C12:0, C7:1, C9:1, C12:1, C8:2, C10:2, C11:2, C12:2, and C14:2. Although some of these urinary acylcarnitines (e.g., Phe-C4:1, Phe-C4:0, and odd-carbon chain acylcarnitines) were probably from diets and gut microbiota [46], their sources and functions clearly warrant further investigations.
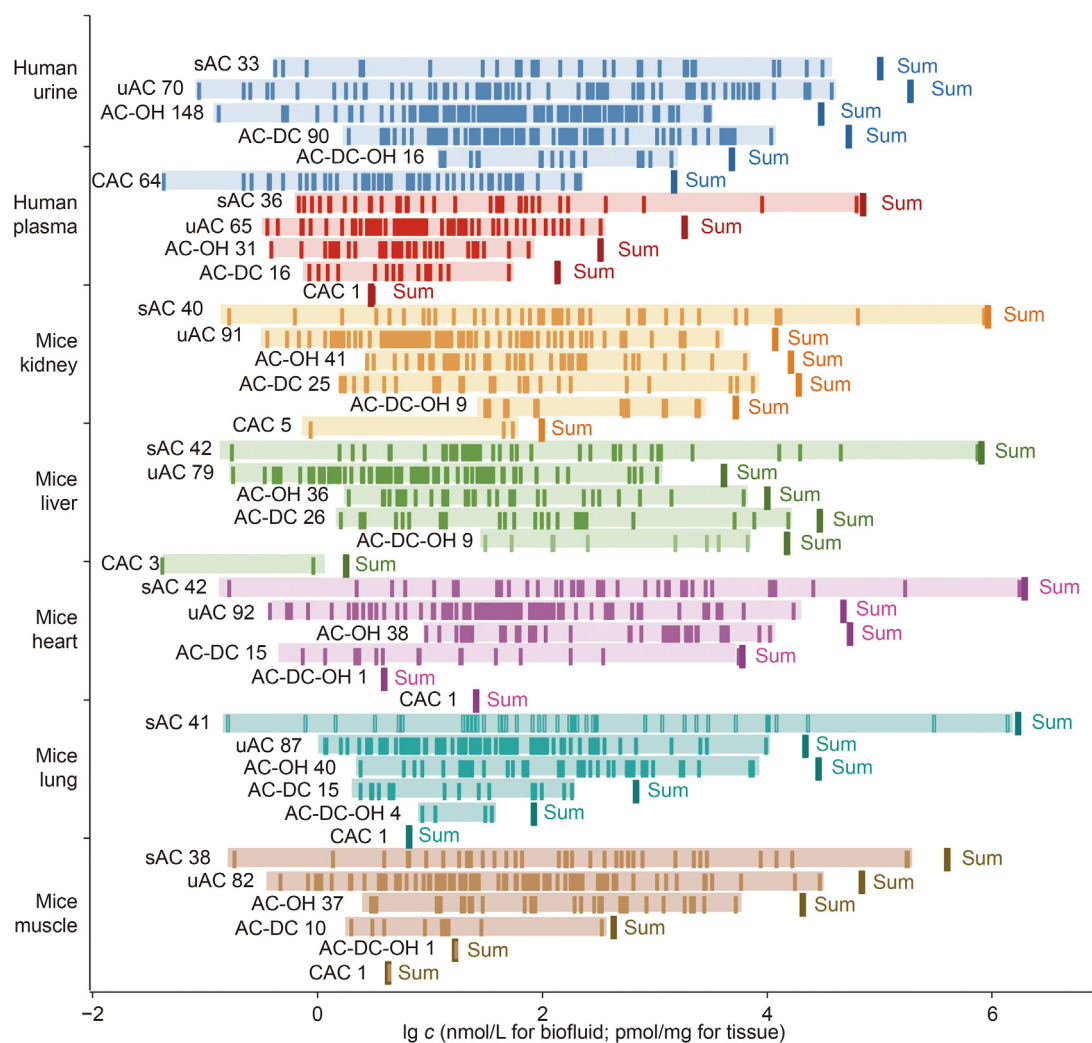

Fig. 5. Concentration (*c*) in multiple biological matrices for acylcarnitine species and different types of acylcarnitines with saturated (sAC), unsaturated (uAC), hydroxylated (AC-OH), carboxylated (AC-DC) chains, and conjugated acylcarnitine (CAC) with bold line (sum) and thin lines indicating total concentration of each class and each species.

Additionally, acylcarnitines had a huge concentration range from 0.31 nM (butenoylcarnitine) to 58.73 μM (carnitine) in human plasma and even greater range in other samples (Fig. 5 and Table S8). The abundances of acylcarnitines also differed greatly in two human biofluids (urine and plasma). For example, the concentration of isobutyrylcanitine (2-M-C3:0) in urine was 164 times higher than in plasma. In contrast, butyrylcarnitine (C4:0) and valerylcarnitines were not detected in urine but abundant in human plasma and all mouse tissues. The acylcarnitine compositions further showed obvious diversities for these mice tissues in terms of different acylcarnitines with the levels ranging from 0.14 pmol/mg (C9:0 and C11:0) to 1.66 μmol/mg (carnitine). Kidney had more acylcarnitine species especially conjugated ones with unsaturated and hydroxylated acyl-chains than the other tissues. In heart and lung tissues, the levels of carnitine (1.3–1.6 μmol/mg) and γ-butyrobetaine (21–24 nmol/mg) were about twice as high as in the other three tissues, whilst acetylcarnitine levels in heart, lung, and muscle tissues (0.16–0.29 μmol/mg) were three times higher than in the other two tissues (0.04–0.06 μmol/mg). These acylcarnitines are broadly attributable to oxidation of fatty acids and branched-chain amino acids in mitochondria and peroxisomes, although the functions of all these detected acylcarnitines warrant further investigations.

Numerous acylcarnitine isomers were concurrently detected in this study although they could be derived from completely different metabolic pathways. Amongst isomers for acylcarnitines with five acyl-carbons, for example, 2-methylbutyrylcarnitine and iso-valerylcarnitine are from isoleucine (Ile) and leucine (Leu) metabolism, respectively, whereas pivaloylcarnitine and valerylcarnitine are adducts of exogenous metabolites pivalic acid and valeric acid, respectively, originated from antibodies [47], microbes [48], and plants [49]. Interestingly, both 2-methylbutyrylcarnitine and iso-valerylcarnitine from two essential amino acids (Ile and Leu) had low levels in all mouse tissues. Hydroxyisobutyrylcarnitine and 3-hydroxybutyrylcarnitine are two isomers but derived from valine and β-hydroxybutyrate, respectively [4,50]. The former had high concentration in heart, lung, and muscle, whereas the latter had high concentration in heart, lung, kidney, and liver (Fig. S11). Apparently, new strategies are required to ambiguously assign these acylcarnitines detected but with no standards.

Moreover, obvious level differences were observable for acylcarnitines in human blood plasma and serum from the same blood sample (Fig. S12). The concentrations of most acylcarnitines were lower in serum than in plasma, including about 80% acylcarnitines with short chains and very long chains as well as 60%–70% acylcarnitines with medium chains and long chains. Therefore, plasma samples are recommended for metabolomic studies of acylcarnitines.

4. Conclusions

We developed a high-throughput UPLC-MS method and detected several hundred acylcarnitines and conjugated acylcarnitines in tested multiple biological matrices with their typical fragment ions recorded. Based on the experimental data from our method, we built a good quality model of QSSR for predicting the t_R values of acylcarnitines with no standards. We also established MRM parameters (t_R, MRM ion pairs, and collision energy) to enable simultaneous quantification of 1136 acylcarnitines using a 10-min UPLC-MS/MS method with good linearity, accuracy, precision, stability, and inter-technician consistency. To the best of our knowledge, this method has the higher coverage and throughput than reported methods. By using this method, moreover, we managed to quantify more than 500 acylcarnitine species in two human biofluids and five mouse tissues offering data for molecular phenotyping these biological matrices. This provides some essential basic biochemical data for these biological matrices and a high-throughput method to quantify acylcarnitines for large cohort studies, which are already ongoing in our lab for various diseases.

CRediT author statement

Jingxian Zhang: Conceptualization, Methodology, Validation, Formal analysis, Investigation, Data curation, Visualization, Writing - Original draft preparation; **Qinsheng Chen:** Validation, Formal analysis, Visualization, Writing - Original draft preparation; **Lianglong Zhang:** Validation, Formal analysis; **Biru Shi:** Validation; **Men Yu:** Conceptualization, Validation; **Qingxia Huang:** Conceptualization, Methodology, Validation, Formal analysis, Investigation, Data curation, Visualization, Writing - Original draft preparation; **Huiru Tang:** Resources, Conceptualization, Methodology, Validation, Formal analysis, Investigation, Data curation, Visualization, Writing - Reviewing and Editing, Supervision, Funding acquisition, Project administration.

Declaration of competing interest

The authors declare that there are no conflicts of interest.

Acknowledgments

Appendix A. Supplementary data

Supplementary data to this article can be found online at https://doi.org/10.1016/j.jpha.2023.10.004.

References

[1] L.L. Jones, D.A. McDonald, P.R. Borum, Acylcarnitines: Role in brain, Prog. Lipid Res. 49 (2010) 61–75.

[2] P.P. Van Veldhoven, Biochemistry and genetics of inherited disorders of peroxisomal fatty acid metabolism, J. Lipid Res. 51 (2010) 2863–2895.

[3] Q. Qu, F. Zeng, X. Liu, et al., Fatty acid oxidation and carnitine palmitoyl-transferase I: Emerging therapeutic targets in cancer, Cell Death Dis. 7 (2016), e2226.

[4] C.B. Newgard, J. An, J.R. Bain, et al., A branched-chain amino acid-related metabolic signature that differentiates obese and lean humans and contributes to insulin resistance, Cell Metab. 9 (2009) 311–326.

[5] P. Negro, F. Gossetti, M. La Pinta, et al., The effect of L-carnitine, administered through intravenous infusion of glucose, on both glucose and insulin levels in healthy subjects, Drugs Exp. Clin. Res. 20 (1994) 257–262.

[6] C.B. Newgard, Metabolomics and metabolic diseases: Where do we stand? Cell Metab. 25 (2017) 43–56.

[7] R.J.A. Wanders, G. Visser, S. Ferdinandusse, et al., Mitochondrial fatty acid oxidation disorders: Laboratory diagnosis, pathogenesis, and the complicated route to treatment, J. Lipid. Atheroscler. 9 (2020) 313–333.

[8] M.M. Adeva-Andany, I. Calvo-Castro, C. Fernández-Fernández, et al., Significance of L-carnitine for human health, IUBMB Life 69 (2017) 578–594.

[9] M. Dambrova, M. Makrecka-Kuka, J. Kuka, et al., Acylcarnitines: Nomenclature, biomarkers, therapeutic potential, drug targets, and clinical trials, Pharmacol. Rev. 74 (2022) 506–551.

[10] J.K. Reddy, T. Hashimoto, Peroxisomal beta-oxidation and peroxisome proliferator-activated receptor alpha: An adaptive metabolic system, Annu. Rev. Nutr. 21 (2001) 193–230.

[11] D. Yu, L. Zhou, Q. Xuan, et al., Strategy for comprehensive identification of acylcarnitines based on liquid chromatography-high-resolution mass spectrometry, Anal. Chem. 90 (2018) 5712–5718.

[12] X. Yan, S.P. Markey, R. Marupaka, et al., Mass spectral library of acylcarnitines derived from human urine, Anal. Chem. 92 (2020) 6521–6528.

[13] M. Guasch-Ferré, M. Ruiz-Canela, J. Li, et al., Plasma acylcarnitines and risk of type 2 diabetes in a Mediterranean population at high cardiovascular risk, J. Clin. Endocrinol. Metab. 104 (2019) 1508–1519.

[14] W. Li, C. Shao, C. Li, et al., Metabolomics: A useful tool for ischemic stroke research, J. Pharm. Anal. 13 (2023) 968–983.

[15] A.S. Koh, F. Gao, J. Liu, et al., Metabolomic profile of arterial stiffness in aged adults, Diab. Vasc. Dis. Res. 15 (2018) 74–80.

[16] J. Mill, V. Patel, O. Okonkwo, et al., Erythrocyte sphingolipid species as biomarkers of Alzheimer's disease, J. Pharm. Anal. 12 (2022) 178–185.

[17] Y. Zhou, Z. Dai, K. Deng, et al., Eight Zhes Decoction ameliorates the lipid dysfunction of nonalcoholic fatty liver disease using integrated lipidomics, network pharmacology and pharmacokinetics, J. Pharm. Anal. 13 (2023) 1058–1069.

[18] K. Enooku, H. Nakagawa, N. Fujiwara, et al., Altered serum acylcarnitine profile is associated with the status of nonalcoholic fatty liver disease (NAFLD) and NAFLD-related hepatocellular carcinoma, Sci. Rep. 9 (2019), 10663.

[19] E.C. Randall, B.G.C. Lopez, S. Peng, et al., Localized metabolomic gradients in patient-derived xenograft models of glioblastoma, Cancer Res. 80 (2020) 1258–1267.

[20] A. Maguolo, G. Rodella, A. Dianin, et al., Diagnosis, genetic characterization and clinical follow up of mitochondrial fatty acid oxidation disorders in the new era of expanded newborn screening: A single centre experience, Mol. Genet. Metab. Rep. 24 (2020), 100632.

[21] A. Ribel-Madsen, R. Ribel-Madsen, C. Brøns, et al., Plasma acylcarnitine profiling indicates increased fatty acid oxidation relative to tricarboxylic acid cycle capacity in young, healthy low birth weight men, Phys. Rep. 4 (2016), e12977.

[22] T. Teav, H. Gallart-Ayala, V. van der Velpen, et al., Merged targeted quantification and untargeted profiling for comprehensive assessment of acylcarnitine and amino acid metabolism, Anal. Chem. 91 (2019) 11757–11769.

[23] G. Theodoridis, H.G. Gika, I.D. Wilson, Mass spectrometry-based holistic analytical approaches for metabolite profiling in systems biology studies, Mass Spectrom. Rev. 30 (2011) 884–906.

[24] S. Chen, H. Kong, X. Lu, et al., Pseudotargeted metabolomics method and its application in serum biomarker discovery for hepatocellular carcinoma based on ultra high-performance liquid chromatography/triple quadrupole mass spectrometry, Anal. Chem. 85 (2013) 8326–8333.

[25] R.W. Jiang, K. Jaroch, J. Pawliszyn, Solid-phase microextraction of endogenous metabolites from intact tissue validated using a Biocrates standard reference method kit, J. Pharm. Anal. 13 (2023) 55–62.

[26] P. Giesbertz, J. Ecker, A. Haag, et al., An LC-MS/MS method to quantify acylcarnitine species including isomeric and odd-numbered forms in plasma and tissues, J. Lipid Res. 56 (2015) 2029–2039.

[27] P.E. Minkler, M.S. Stoll, S.T. Ingalls, et al., Validated method for the quantification of free and total carnitine, butyrobetaine, and acylcarnitines in biological samples, Anal. Chem. 87 (2015) 8994–9001.

[28] L. Sun, L. Liang, X. Gao, et al., Early prediction of developing type 2 diabetes by plasma acylcarnitines: A population-based study, Diabetes Care 39 (2016) 1563–1570.

[29] L. Xiang, J. Wei, X.Y. Tian, et al., Comprehensive analysis of acylcarnitine species in db/db mouse using a novel method of high-resolution parallel reaction monitoring reveals widespread metabolic dysfunction induced by diabetes, Anal. Chem. 89 (2017) 10368–10375.

[30] T. Tang, P. Zhang, S. Li, et al., Absolute quantification of acylcarnitines using integrated Tmt-PP derivatization-based LC-MS/MS and quantitative analysis of multi-components by a single marker strategy, Anal. Chem. 93 (2021) 12973–12980.

[31] Y. Wen, R.I.J. Amos, M. Talebi, et al., Retention index prediction using quantitative structure-retention relationships for improving structure identification in nontargeted metabolomics, Anal. Chem. 90 (2018) 9434–9440.

[32] Q. Hu, Y. Sun, P. Yuan, et al., Quantitative structure-retention relationship for reliable metabolite identification and quantification in metabolomics using ion-pair reversed-phase chromatography coupled with tandem mass spectrometry, Talanta 238 (2022), 123059.

[33] A.A. D'Archivio, M.A. Maggi, F. Ruggieri, Modelling of UPLC behaviour of acylcarnitines by quantitative structure-retention relationships, J. Pharm. Biomed. Anal. 96 (2014) 224–230.

[34] C. Feng, L. Xue, D. Lu, et al., Novel strategy for mining and identification of acylcarnitines using data-independent-acquisition-based retention time prediction modeling and pseudo-characteristic fragmentation ion matching, J. Proteome Res. 20 (2021) 1602–1611.

[35] U.S. Food and Drug Administration, Bioanalytical Method Validation Guidance for Industry. https://www.fda.gov/regulatory-information/search-fda-guidance-documents/bioanalytical-method-validation-guidance-industry. (Accessed 24 May 2018).

[36] M. Aschi, A.A. D'Archivio, M.A. Maggi, et al., Quantitative structure-retention relationships of pesticides in reversed-phase high-performance liquid chromatography, Anal. Chim. Acta 582 (2007) 235–242.

[37] K.P. Singh, S. Gupta, A. Kumar, et al., Linear and nonlinear modeling approaches for urban air quality prediction, Sci. Total Environ. 426 (2012) 244–255.

[38] M. Peng, X. Fang, Y. Huang, et al., Separation and identification of underivatized plasma acylcarnitine isomers using liquid chromatography-tandem mass spectrometry for the differential diagnosis of organic acidemias and fatty acid oxidation defects, J. Chromatogr. A 1319 (2013) 97–106.

[39] L. Vernez, G. Hopfgartner, M. Wenk, et al., Determination of carnitine and acylcarnitines in urine by high-performance liquid chromatography-electrospray ionization ion trap tandem mass spectrometry, J. Chromatogr. A 984 (2003) 203–213.

[40] A. Zuniga, L. Li, Ultra-high performance liquid chromatography tandem mass spectrometry for comprehensive analysis of urinary acylcarnitines, Anal. Chim. Acta 689 (2011) 77–84.

[41] F. Wang, L. Sun, Q. Sun, et al., Associations of plasma amino acid and acylcarnitine profiles with incident reduced glomerular filtration rate, Clin. J. Am. Soc. Nephrol. 13 (2018) 560–568.

[42] The Human Metabolome Database. https://hmdb.ca/. (Accessed 1 January 2022).

[43] A.K. Bhaskar, S. Naushin, A. Ray, et al., A high throughput lipidomics method using scheduled multiple reaction monitoring, Biomolecules 12 (2022), 709.

[44] C. Hellmuth, M. Weber, B. Koletzko, et al., Nonesterified fatty acid determination for functional lipidomics: Comprehensive ultrahigh performance liquid chromatography-tandem mass spectrometry quantitation, qualification, and parameter prediction, Anal. Chem. 84 (2012) 1483–1490.

[45] L.M. Hall, D.W. Hill, K. Bugden, et al., Development of a reverse phase HPLC retention index model for nontargeted metabolomics using synthetic compounds, J. Chem. Inf. Model. 58 (2018) 591–604.

[46] K. Weitkunat, C.A. Bishop, M. Wittmüss, et al., Effect of microbial status on hepatic odd-chain fatty acids is diet-dependent, Nutrients 13 (2021), 1546.

[47] E.P. Brass, Pivalate-generating prodrugs and carnitine homeostasis in man, Pharmacol. Rev. 54 (2002) 589–598.

[48] T. Rezanka, L. Siristova, O. Schreiberová, et al., Pivalic acid acts as a starter unit in a fatty acid and antibiotic biosynthetic pathway in *Alicyclobacillus*, *Rhodococcus* and *Streptomyces*, Environ. Microbiol. 13 (2011) 1577–1589.

[49] F. Peng, L. Sheng, B. Liu, et al., Comparison of different extraction methods: Steam distillation, simultaneous distillation and extraction and headspace co-distillation, used for the analysis of the volatile components in aged flue-cured tobacco leaves, J. Chromatogr. A 1040 (2004) 1–17.

[50] M.R. Soeters, M.J. Serlie, H.P. Sauerwein, et al., Characterization of D-3-hydroxybutyrylcarnitine (ketocarnitine): An identified ketosis-induced metabolite, Metabolism 61 (2012) 966–973.